Helium effects on displacement cascades in α-iron

2008 J. Phys.: Condens. Matter 20 415206

(http://iopscience.iop.org/0953-8984/20/41/415206)

J. Phys.: Condens. Matter **20** (2008) 415206 (12pp) doi:10.1088/0953-8984/20/41/415206

Helium effects on displacement cascades in α-iron

G Lucas and R Schäublin

Ecole Polytechnique Fédérale de Lausanne (EPFL), Centre de Recherche en Physique des Plasmas, Association Euratom-Confédération Suisse, CH-5332 Villigen PSI, Switzerland

E-mail: guillaume.lucas@psi.ch

Received 4 July 2008, in final form 20 August 2008
Published 12 September 2008
Online at stacks.iop.org/JPhysCM/20/415206

Abstract

Molecular dynamics simulations have been performed to investigate the effects of helium on the displacement cascades in α-iron. Besides conventional analysis tools, a new graphical representation of the data based on ternary plots has been introduced. Results show that the production of defects and their subsequent clustering appear to be greatly influenced by the presence of helium. Calculations reveal that the location of helium atoms, substitutional or interstitial, plays a major role. Compared to pure iron, interstitial helium atoms increase the amount of Frenkel pairs generated during the cascades. Conversely, substitutional helium atoms tend to decrease this production. However, in both cases, it is observed that helium atoms stabilize larger self-interstitial clusters, due to a strong binding energy. These simulations show that helium atoms trap self-interstitial clusters and would thus slow down their subsequent migration. Some helium–vacancy clusters are generated in the core of the displacement cascades but also grow at the periphery of self-interstitial clusters. It is shown that results greatly depend on the irradiation temperature.

(Some figures in this article are in colour only in the electronic version)

1. Introduction

Ferritic steels are possible structural materials for future fusion reactors. During the operation of these reactors, materials are subjected to 14 MeV neutron irradiation, generating helium by transmutation reactions and simultaneously energetic displacement damage. High helium concentrations are known to induce the formation of He bubbles and consequently enhance void swelling. Helium may also modify the evolution of the microstructure, leading to undesirable phenomena such as high temperature embrittlement [1]. These deteriorations may result from the insolubility of He, which therefore tends to precipitate into vacancies, voids or grain boundaries [2–4].

Experimental and theoretical investigations are performed to model the undesirable irradiation effects on the mechanical properties in fusion reactor materials [5], with a significant effort solely dedicated to displacement cascades [6]. Some experiments in metal implanted with helium at intermediate temperatures to relatively high concentrations provided clear evidence that He atoms can be efficiently resolved from small bubbles by displacement cascades, resulting in the nucleation of secondary generation bubbles [7]. Despite this problem having already been discussed [8] and an analytic model proposed [9], the details of this process are presently not well understood. At the atomic scale, theoretical studies provide useful information on the energetics, the diffusion and the interaction of helium atoms with point defects, dislocations or grain boundaries [10, 11]. On the basis of atomistic results, and the guidance of helium desorption experiments, the role of helium in the evolution of the microstructure has been recently studied using kinetic Monte Carlo (KMC) [12]. As already noticed [13], this study has pointed out the necessity to include traps for self-interstitial clusters in order to reproduce the experimental data. The nature of these traps still remains unknown.

Up to now, few studies have been dedicated to study the interaction of helium atoms with displacement cascades. In recent years some molecular dynamic simulations have shown the clustering of small helium–vacancy clusters within displacement cascades [14, 15] and another one the influence of helium on the clustering of self-interstitial clusters [16]. The purpose of this paper is to investigate in more detail the effects of helium on the displacement cascades by means of molecular dynamics simulations, in particular the influence of

helium atoms on the formation of self-interstitial clusters and the possible nucleation of He bubbles. To understand these effects the results of the generated cascades have been carefully analyzed to extract the production of Frenkel pairs and relevant information on the clustering of self-interstitial atoms (SIA) and helium atoms with vacancies or SIAs. As a matter of fact, in a real material helium atoms are easily trapped into grain boundaries or vacancies, but they should also be easily redissolved in the matrix ballistically by the displacement cascades [9]. For such a reason, both substitutional and interstitial helium atoms have been considered in this study. The amount of helium atoms introduced in the simulations ranges from 0.1 to 1.0 at.% (1000–10 000 appm). This represents roughly the amount of helium which should be found in a fusion reactor material at the end of its life, after 50–100 displacements per atom (dpa) [17]. It can be seen as a very large helium content but, due to space- and timescales, reachable by MD simulation such high concentrations are still mandatory to exhibit the effects of helium.

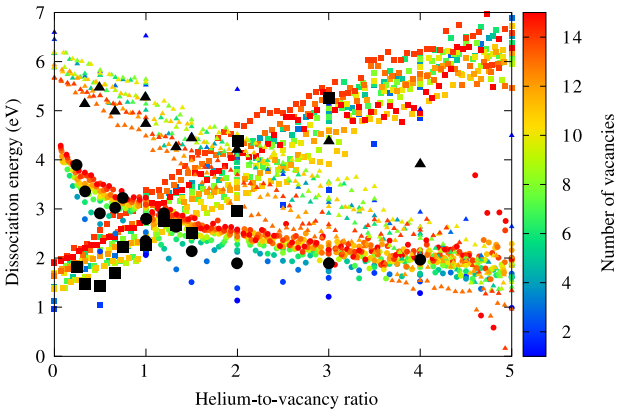

Figure 1. Dissociation energies in eV of a vacancy (square), a helium interstitial (circle) and a self-interstitial atom (triangle) from an He_nV_m cluster as a function of the helium-to-vacancy ratio n/m, calculated with the Ackland potential [20], Beck potential [21] and Juslin potential [22], respectively, for the Fe–Fe, He–He and Fe–He interactions. The black symbols correspond to the data obtained using density functional theory by Fu *et al* [10, 23].

2. Computational method

2.1. Molecular dynamics settings

Simulations have been performed using the modified molecular dynamics code MOLDY [18]. The box size was set to $63a_0 \times 63a_0 \times 63a_0$ (∼500 000 atoms). For all simulations periodic boundary conditions and a constant volume were used. A variable timestep, no higher than 1 fs, have been used for all simulations. The temperature of the system was controlled every hundred timesteps by a velocity rescaling algorithm applied on two atomic layers on each side of the simulation cell. Three different temperatures have been used, i.e. 10, 300 and 523 K. Particular attention has been given to the original location of the helium, that is to say if the He is initially interstitial or substitutional. Moreover two different contents of He have been studied: 0.1 and 1.0 at.%, initially randomly distributed in the simulation box. The primary knocked-on atom (PKA) energies ranged between 3 and 20 keV. For each identical initial condition, 20 cascades with randomly chosen PKA directions have been carried out. After an equilibration period of about 2 ps, the evolution of the system is monitored during 25 ps. The final configuration is then relaxed using a conjugate gradient algorithm. Considering all the parameters we varied, more than 1200 cascades have been performed. Each cascade was followed by a defect and a cluster analysis as described below.

2.2. Choice of empirical potentials

The choice of the empirical potential is based on a comparative study of the formation of He_nV_m clusters in iron [19]. According to this study, He_nV_m clusters are better described when the Ackland potential [20] and Beck potential [21] are used to describe, respectively, Fe–Fe and He–He interactions, in combination with a recent potential developed by Juslin *et al* for Fe–He interactions [22].

Despite the well-known drawbacks of the Ackland potential in the description of formation and migration energies of self-interstitials (SIAs) in iron, this combination of potentials seems more adequate to deal with simulations involving helium atoms. Figure 1 shows the dissociation energies of a vacancy, a helium interstitial and a self-interstitial atom from an He_nV_m cluster as a function of the helium-to-vacancy ratio n/m, calculated with this set of potentials. These energies are compared to the ones obtained by *ab initio* calculations within the density functional theory [10, 23]. *Ab initio* calculations on small He_nV_m clusters (n and m up to 4) have pointed out that the crossover corresponding to the intersection of the dissociation energy curves for helium and vacancy should occur for a ratio n/m around 1.3 and a dissociation energy around 2.6 eV. According to our calculations [19], the Juslin potential seems more adequate than the Wilson–Johnson potential [24] to describe this optimal ratio, although it underestimates it a bit. Other recent DFT calculations have shown that the dissociation energy of SIAs remains high even for high helium content [23]. Hence only the Juslin potential associated with the Ackland potential gives satisfactory results concerning this issue, the loop-punching regime appearing for n/m ratio above 4–5 depending on the number of vacancies in the cluster. Contrary to the Wilson–Johnson potential, the Juslin potential predicts that the tetrahedral He interstitial is more stable than the octahedral He interstitial, in agreement with *ab initio* calculations on formation energies of interstitial He [10]. The combination of potentials presented in this paper compares fairly well with the DFT calculations and seems particularly adequate to describe helium–vacancy clusters.

2.3. Analysis methods

2.3.1. Defects analysis. The analysis is based on the decomposition of the simulation cell in Wigner–Seitz cells using a reference perfect crystal. The Wigner–Seitz cell around a lattice point is defined as the locus of points in space, which are closer to that lattice point than to any of the other

lattice points. Once this decomposition is done, the atoms contained in each Wigner–Seitz cell are counted. If no atom is found within a Wigner–Seitz cell, we consider one vacancy. If one iron atom is found, we consider a substitutional iron (or replacement). When the Wigner–Seitz cell contains two iron atoms or more, one of the iron atoms is considered as substitutional and the other as interstitial. In the case when only helium atoms are found, it is considered that there is one vacancy that is filled by helium. These considerations can be easily summarized for any number and type of atoms contained within a Wigner–Seitz cell by considering whether or not it contains iron atoms:

$$\begin{aligned} n_{\mathrm{Fe}} = 0 \Rightarrow n_{\mathrm{V}} = 1; \qquad & n_{\mathrm{Fe}_i} = 0 \\ n_{\mathrm{Fe}} \neq 0 \Rightarrow n_{\mathrm{V}} = 0; \qquad & n_{\mathrm{Fe}_i} = n_{\mathrm{Fe}} - 1, \end{aligned} \tag{1}$$

where n_{Fe} is the number of iron atoms contained within the Wigner–Seitz cell, n_{Fe_i} is the number of interstitial irons and n_{V} is the number of vacancies.

2.3.2. Pair distance correlation functions. A usual manner to characterize the spatial correlation between atoms in a medium containing N atoms is the well-known radial distribution function $g(r)$, which gives the pair correlation as a function of the distance r between pairs of atoms [25]. In this study, we are only interested in the defects formed during displacement cascades. Given their limited sizes and their irregular shapes, it has been shown useful to use the so-called pair distance correlation function (pdf) [26] defined as

$$G(r) = \frac{1}{N(N-1)} \sum_{i=1}^{N} \sum_{j=1}^{N} \delta(r - r_{ij}). \tag{2}$$

In a homogeneous medium $G(r)$ increases with r^2. It is often more useful to use instead the integrated pair distance correlation function

$$IG(R) = \int_0^R G(r)\,\mathrm{d}r. \tag{3}$$

This function is normalized in the case of displacement cascades as it reaches unity when $R \geqslant R_{ij}^{\max}$, the largest distance between two defects in a cascade.

2.3.3. Cluster size analysis. An analysis based on a simple radius criterion has been performed to study the size and the nature of the clusters remaining after the displacement cascades. If two defects are closer than a given cutoff radius, they belong to the same cluster. Arbitrarily, each cutoff radius is chosen such as the binding energy between two species above this radius is less than 20% of the maximum binding energy. For instance, the maximum binding energy for two self-interstitials is found to be around 1.2 eV when they are closer than $1a_0$. Above $1.5a_0$, for all possible configurations, their binding energy decreased below 20% of its maximal value, i.e. ∼0.25 eV, and this separation distance is thus set as the cutoff radius between these two species. The considered species used to determine the radii were the Fe self-interstitial, the vacancy and the He interstitial in tetrahedral position. The related cutoff radii used for the analysis are summarized in table 1.

Table 1. Cutoff radii r_c in a_0 used for the cluster analysis. See the text for details.

	$\mathrm{Fe_{int}}$	V	He
$\mathrm{Fe_{int}}$	1.50	1.00	1.50
V	1.00	1.25	1.25
He	1.50	1.25	1.25

2.3.4. Cluster composition analysis. We propose an original way, based on a new ternary plot, to qualitatively assess the effects of helium on displacement cascades. It graphically depicts for a cluster the ratios of the three defect species, i.e. helium, vacancy and SIA, as a single position in an equilateral triangle. Every species is represented by a corner of the triangle. In the ternary plot, the sum of the relative proportion of the considered defect species represents 100%. Because this sum is constant for all clusters being plotted, any one proportion is not independent of the others, so only two proportions must be known to find a point and the intersection of the three proportions has thus two dimensions in this graph. Each base of the triangle represents a proportion of a given species of 0%, while the corner of the triangle opposite to that base represents a proportion of 100%. When a given proportion increases in any one cluster, the point representing that cluster moves from the base to the opposite point of the triangle. Additional information on a cluster is then added to this diagram. The size of the disc used to mark its position is proportional to the size of the cluster. Moreover the occurrence of a certain cluster size and composition is depicted using a color scale. This representation allows us to characterize in one glance the nature, size and frequency of the clusters formed during the displacement cascades.

3. Results

3.1. Point defect production

Figure 2 shows the number of Frenkel pairs N_{FP} given by the number of interstitial Fe atoms created by the displacement cascades as a function of the kinetic energy of the PKA at 10 K, 300 K and 523 K. Each data point at a given energy results from the averaging of 20 cascades. As a guideline, for each He content the data points have been fitted using a power law $N_{\mathrm{FP}} = A(E_{\mathrm{PKA}})^m$, as proposed by Bacon *et al* [27]. In pure Fe, the effect of the irradiation temperature is weak as the temperature increases from 10 to 523 K. A slight decrease of the number of Frenkel pairs is observed with increasing irradiation temperature, which is in agreement with previous calculations [27, 15]. From the figures, it can be clearly seen that the presence of helium greatly influences the defect production in iron. For instance, at 300 K, a 10 keV produced on average 24 Frenkel pairs in pure iron. The addition of 1.0 at.% of He interstitials increases the production up to 48 Frenkel pairs per cascade, in contrast to the addition of 1.0 at.% of substitutional He which reduces the production to as low as two Frenkel pairs per cascade. The effect of helium depends thus greatly on its initial position, i.e. interstitial or substitutional. This effect can be explained by the additional

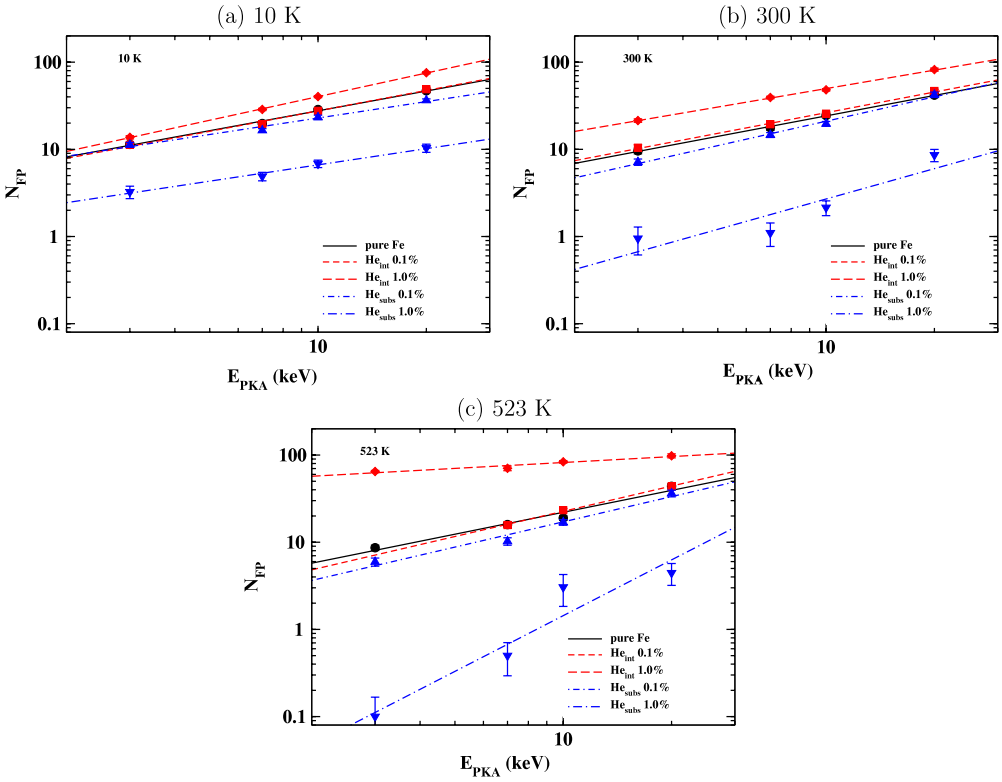

Figure 2. Number of Frenkel pairs N_{FP} as a function of PKA energy E_{PKA} for different He contents and pure α-iron at (a) 10 K, (b) 300 K and (c) 523 K. The bars show the standard errors.

stress induced by He interstitials in the lattice, which may help to kick out a lattice atom in a self-interstitial position. This effect appears more significant for small PKA energies. Conversely, and even if in both cases the effect of He on the production of defects increases with its concentration, the presence of substitutional He atoms induces a lower defect production. Indeed, during a displacement cascade, an Fe interstitial can easily recombine with a substitutional helium by a kick-out mechanism [28], which implies a large energy gain of about 4.6 eV with our set of potentials to be compared with the 3.6 eV obtained by Fu *et al* [23]. This mechanism results in the production of an interstitial He.

The influence of irradiation temperature on the defect production when the material contains He is more significant than in pure iron. In the presence of helium, all observed effects are enhanced by a temperature increase. The high mobility of self-interstitials and interstitial He with increasing temperature could play an important role. In the case of interstitial He, the slope of the fitted line decreases with increasing temperature. It seems that, with temperature, the system reaches saturation faster in the concentration of Frenkel pairs [29, 30]. In contrast in the case of substitutional He, the slope of the fitted line increases from 10 to 523 K.

3.2. Spatial correlation between defects

The integrated pdfs corresponding to SIA–SIA pairs ($IG_{\mathrm{II}}(r)$), vacancy–vacancy pairs ($IG_{\mathrm{VV}}(r)$) and SIA–vacancy pairs ($IG_{\mathrm{IV}}(r)$) are presented in figure 3 for 10 keV displacement

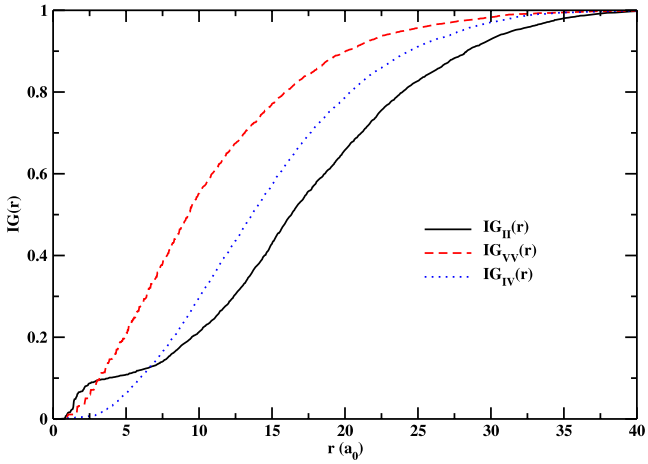

Figure 3. SIA–SIA, vacancy–vacancy and SIA–vacancy integrated pair distance correlation functions for 10 keV cascades at 300 K in pure iron.

cascades at 300 K in pure iron. $IG_{\mathrm{II}}(r)$ displays an excess of pairs at short distances around 1 to 8 a_0, which indicates an aggregation of SIAs. This excess also appeared in $IG_{\mathrm{VV}}(r)$. This is, however, not observed in the case of heterogeneous SIA–vacancy pairs. This is due to the high probability for an SIA and a vacancy to annihilate at close distance. In addition, according to the conventional cascade picture, vacancy and self-interstitials tend to be physically separated with vacancies dominating in the core of the cascade and interstitials at its

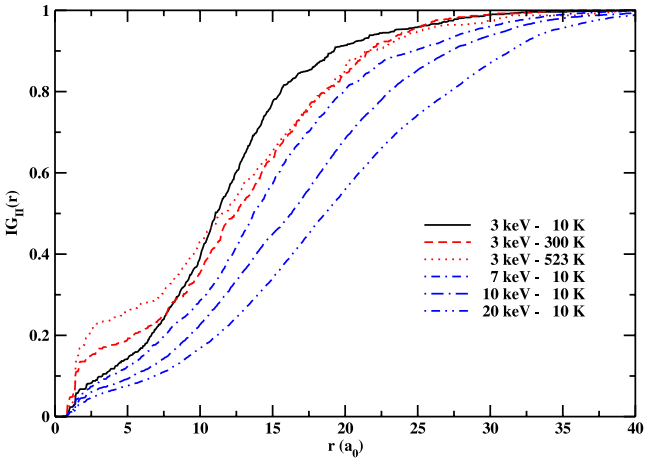

Figure 4. SIA–SIA integrated pair distance correlation functions for several PKA energies and irradiation temperatures in pure iron.

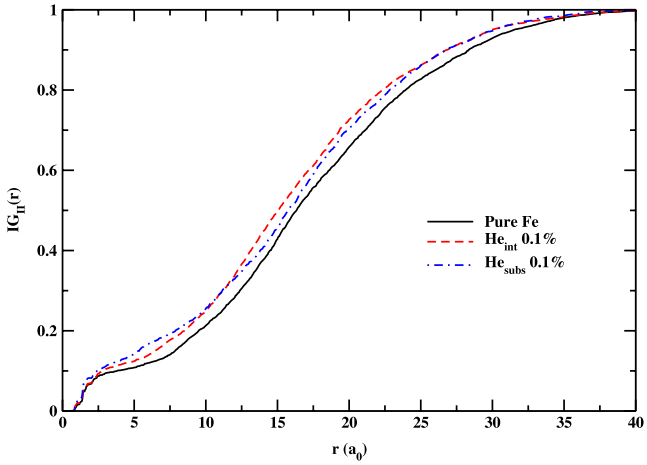

Figure 5. SIA–SIA integrated pair distance correlation functions with different He contents for 10 keV cascades at 300 K.

periphery [31, 27, 32], making small SIA–vacancy separations rather unlikely. The long-range correlation extends further in the case of SIA–SIA pairs compared to vacancy–vacancy pairs, as the half-height position of $IG_{\mathrm{II}}(r)$ is found around $16a_0$ against $9a_0$ for $IG_{\mathrm{VV}}(r)$. This is also consistent with the traditional cascade picture. The same trends are observed when adding He.

Figure 4 shows the integrated pdfs of SIA pairs in pure iron for cascades performed at temperatures ranging from 10 to 523 K and PKA energies from 3 to 20 keV. On the curves resulting from 3 keV cascades, we can see that the temperature mainly affects the short-range correlation between SIA–SIA pairs. The higher the irradiation temperature, the larger the pair excess around 1 to $8a_0$. It clearly indicates the tendency of SIAs to form more numerous and/or larger clusters at high temperature, as observed by others [27]. As the PKA energy increases, the produced defects recoil further from the core of the cascades. As a result, SIA–SIA pair distances are longer on average, which flattens the pdfs. At 10 K, the half-height of the pdfs goes from $\sim 11a_0$ for 3 keV PKA to $\sim 18a_0$ for 20 keV PKA.

Figure 5 presents integrated SIA–SIA pdfs obtained at 300 K for 10 keV cascades with different helium contents. In order to allow a fair comparison with pure iron, only the cases with 0.1 at.% of helium, either interstitial or substitutional, are displayed, as the amount of Frenkel pairs produced are roughly the same as seen in section 3.1. It can be seen that, in the presence of interstitial He, the short-range part of the pdf slightly increases compared to pure iron, especially above $2.5a_0$. This increase seems more evident in the presence of substitutional helium. It may indicate a tendency for helium to favor the formation of larger SIA clusters. The presence of helium also seems to affect the long-range part of the pdf curves as they remain above the curve corresponding to pure iron. This slightly shorter separation of SIA pairs, a few a_0, might be the consequence of a reduction of mobility of SIA clusters induced by the helium.

Figure 6 shows the pdfs corresponding to 10 keV cascades and 1.0 at.% interstitial He at 10, 300 and 523 K. These curves

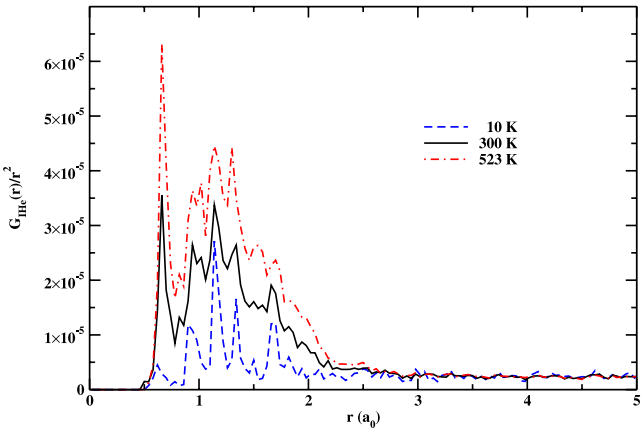

Figure 6. Short-range SIA–helium pair distance correlation functions (divided by r^2) for 1.0 at.% He interstitials for 10 keV cascades at 10, 300 and 523 K.

have been divided by r^2 in order to avoid the random tail resulting from the large quantity of helium still homogeneously distributed in the simulation cell. It must be noticed that with this concentration the average separation between helium is about $3.7a_0$. In all cases it appears that a substantial amount of short-range SIA–helium pairs are formed from $0.5a_0$–$2a_0$. This is strong evidence of the clustering of helium atoms with SIAs. There is clearly an attractive interaction between the helium and the SIAs. The first peak shows that the closest separation between a helium and an SIA or an SIA cluster can be as short as $0.7a_0$. Higher temperatures allows the formation of larger clusters because of the increased mobility of SIAs and the enhanced migration of He interstitials. As a consequence a stronger correlation is found at higher temperature on the pdf curves.

3.3. Cluster size distributions

Figure 7 shows the influence of interstitial He on the SIA clustering for an irradiation temperature of 523 K. As expected, in all cases the number and size of SIA clusters is highly

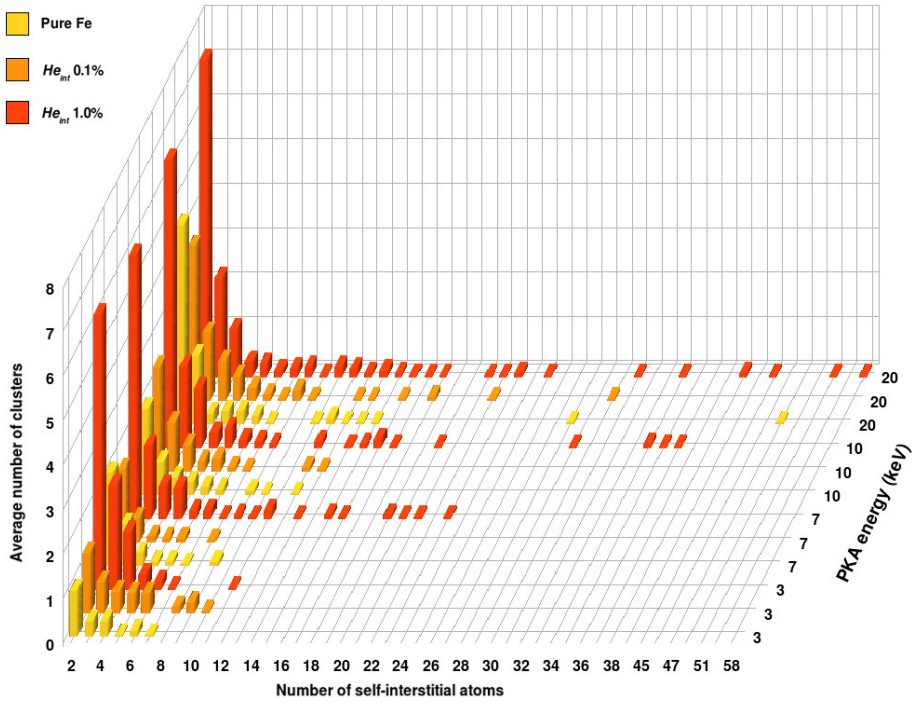

Figure 7. Average size distribution of Fe interstitials in the clusters with initially 0.1 and 1.0 at.% of interstitial He at 523 K as a function of the PKA energy.

dependent on the PKA energy, as it is directly related to the production of Frenkel pairs. With initially 0.1 at.% of interstitial He, the number of SIA clusters seems comparable to the case of pure iron, but their average size increases slightly. With 1.0 at.% of interstitial He, the number and size of SIA clusters increase drastically, the larger SIA cluster containing up to 58 SIAs for the 20 keV cascades. Helium therefore plays a noticeable role in the stabilization of large SIA clusters. This stabilization effect is consistent with a study from Ventelon and coworkers, in which they have calculated strong binding energies between interstitial He atoms and SIA clusters, accompanied by a decrease of their mobility [33].

The effect of substitutional He on the clustering of SIAs is significantly different from the one of interstitial He. As shown in figure 8 for cascades carried out at 523 K, the presence of substitutional He decreases the amount of SIA clusters produced during the cascades, admittedly only slightly at 0.1 at.% helium content but drastically at 1.0 at.% helium content. This effect can be easily rationalized in the following way. During the first stage of a displacement cascade, a substitutional He is easily kicked out from its position to form a vacancy and an interstitial He, as about 2 eV is needed to free the helium atom. Besides, a SIA can subsequently easily recombine with a substitutional He by a kick-out mechanism with a significant energy gain, leaving a free interstitial He. Consequently the number of SIA clusters tends to decrease in the presence of substitutional He, as many potential vacancies are made available for recombination. At 0.1 at.% helium, however, the number of large SIA clusters remains equal or even higher than in pure iron. One can assume here that the interstitial He atoms formed during the cascades can easily migrate and find SIA clusters. Once helium atoms are trapped by these clusters, the latter are in turn stabilized, as observed in the case of 0.1 and 1.0 at.% interstitial He.

3.4. Influence of temperature on the clustering

Temperature plays an important role in the clustering of self-interstitials in iron in the presence of helium. Figure 9 presents the size distribution of SIA clusters for 10 keV cascades at different irradiation temperatures and helium content. In pure iron, as already remarked on the production of Frenkel pairs, the number of SIA clusters slightly decreases from 10 to 523 K. However, in the presence of helium, the irradiation temperature remarkably enhances the effects cited in previous paragraphs, that is to say, on the one hand, in the case of interstitial He more numerous and larger SIA clusters are formed at high temperature, and on the other hand, in the case of substitutional He less numerous SIA clusters are produced. It must be noticed that, at 10 K with 0.1 at.% substitutional He, SIA clusters are much smaller than in the pure iron case. At 300 and 523 K, however, it is the opposite and produced clusters are slightly larger than in pure iron. This observation consolidates the following hypothesis. After helium atoms are detrapped from a substitutional position during the cascade process, interstitial He atoms are available in the simulation cell. As their migration is associated with a very low migration energy of 0.06 eV, they can migrate easily even at relatively low temperatures, but at 10 K they would then be trapped by SIA clusters, which are in turn stabilized due to the strong binding energy with interstitial He atoms. This could explain the difference observed between 10 K and the higher irradiation temperatures.

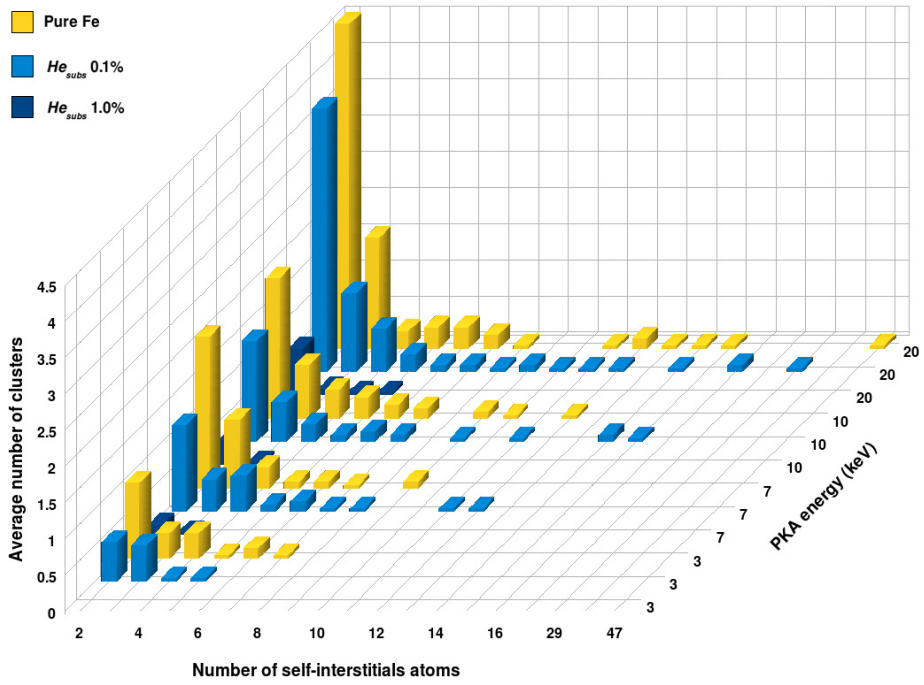

Figure 8. The average size distribution of Fe interstitials in the clusters in iron with initially 0.1 and 1.0 at.% of substitutional He for different PKA energies at 523 K.

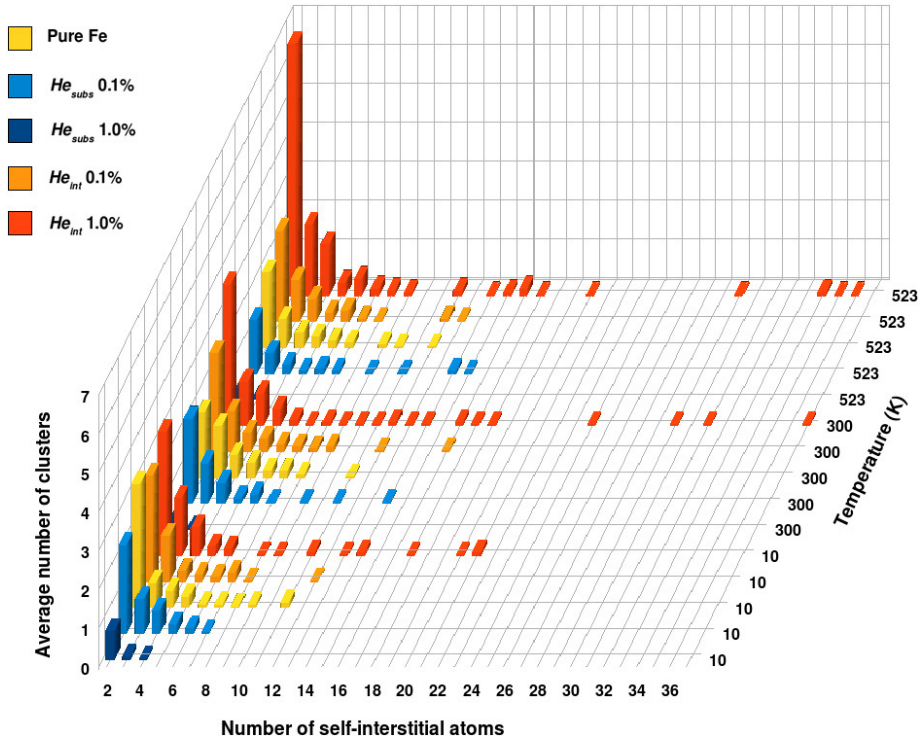

Figure 9. The average size distribution of Fe interstitials in the clusters in iron with different initial helium contents for 10 keV cascades at 10, 300 and 523 K.

3.5. Structure of SIA clusters

The typical structure of large SIA clusters found in our simulations is given in figure 10 for 0.1 and 1.0 at.% of interstitial He. Most SIA clusters are usually formed by self-interstitials mainly aligned in a ⟨111⟩-type direction, often forming, for the larger ones, a platelet on a {110} habit plane. They thus tend to form $\frac{1}{2}a_0\langle 111\rangle\{110\}$ dislocation loops, as has been observed experimentally in pure iron [34] or predicted by MD simulations [35, 36]. More about their orientation will be

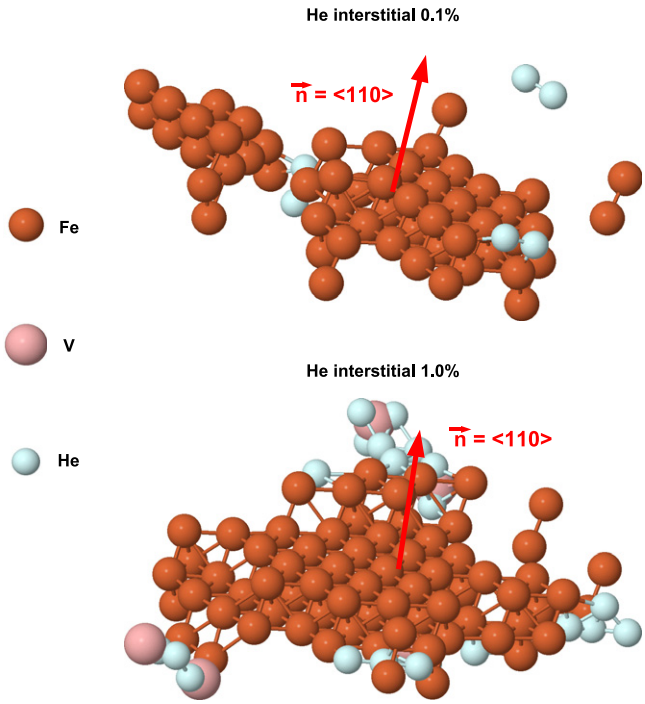

Figure 10. Typical structure of large SIA clusters obtained at 523 K from a 20 keV cascade in iron containing initially 0.1 and 1.0 at.% of He interstitials.

discussed later. Helium atoms never incorporate the core of the loop, but instead surround the SIA clusters, forming small He_n or He_nV_m clusters. The latter type of cluster is rarely encountered with 0.1 at.% helium but is common with 1.0 at.% of helium. The density of helium in these He_nV_m clusters is very high, probably high enough to initiate loop punching [37], which provides an additional source for the observed growth of SIA clusters in high helium concentration conditions. It must be noted that He_n clusters are preferentially located at the periphery of the SIA clusters in the loop plane where there is a tensile strain field, whereas He_nV_m clusters do not really seem to have a preferential location, which is consistent with the work of Shim *et al* on the interaction between SIA dislocation loops and He in bcc iron [38].

3.6. Structure of He_nV_m clusters

During the displacement cascades a significant amount of helium–vacancy clusters are formed. In the case of iron containing interstitial He, these He_nV_m clusters can have n/m ratios close to 1 and can even reach high helium densities, up to a ratio of 5 for a high concentration of helium, especially when nucleated around an SIA cluster as discussed above. In the case of iron containing substitutional He, the He_nV_m clusters usually have a lower n/m ratio and rather large clusters can be homogeneously nucleated within the cascades at high concentrations. Figure 11 shows the largest He_nV_m cluster among all simulations. It occurred for a high content of substitutional He, i.e. 1.0 at.%, at 300 K for a 20 keV PKA energy. This cluster contains 40 vacancies and 9 helium atoms and, as for most of the large clusters, the n/m ratio is below 1.

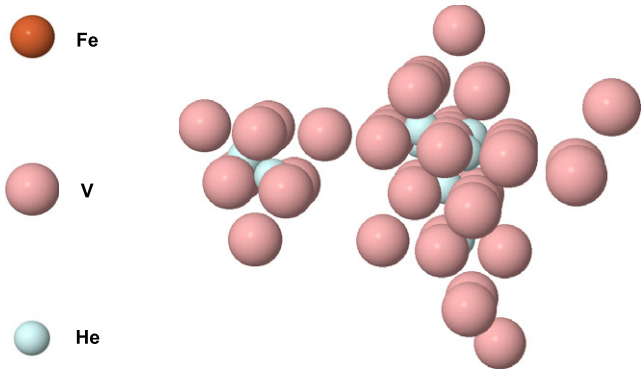

Figure 11. He_9V_{40} cluster formed at 300 K in a 20 keV cascade in iron containing initially 1.0 at.% of substitutional He.

4. Discussion

4.1. Composition of the clusters

It appears that the overall composition of the clusters resulting from the displacement cascades is greatly influenced by the amount and the location, interstitial or substitutional, of the helium, which could in fact seriously impact the subsequent thermal aging and microstructural evolution of the material, in particular He bubble nucleation and growth.

Average composition of the clusters remaining after 10 keV displacement cascades at 300 K for samples containing no helium, 0.1 at.% of interstitial He and 0.1 at.% of substitutional He is given in figure 12 using ternary plots. In pure iron, as seen on the Fe–V axis, some of the SIA clusters contain a few vacancies. These vacancies are likely to annihilate within a short period [26]. However, vacancies and SIAs tend to be physically separated, with vacancies dominating in the core of cascades and SIAs at the periphery [31, 32].

With 0.1 at.% of interstitial He, a large number of SIA clusters remaining after the cascades are accompanied by interstitial He atoms. This can be seen on the Fe–He axis on the corresponding ternary plot. With a higher content of interstitial He, most of the SIA clusters are surrounded by these interstitial He atoms. This clearly indicates that a heterogeneous nucleation of He bubbles is favored. Besides, there is an obvious size increase of the SIA clusters induced by the presence of helium. As already discussed in the previous section, there is an argument in favor of this observation. The interstitial He atoms have strong binding energies with SIA clusters, of the order of 1.2–1.4 eV [33], which result in their trapping at the periphery of the SIA clusters. It can also be noted in the He–V axis that numerous interstitial He atoms fill the newly formed vacancies to form small He_nV_m clusters with an n/m ratio increasing accordingly to the amount of initial interstitial He.

In the case of substitutional He, the composition of clusters changes slightly at low content. The main difference compared to the case where helium is initially in an interstitial position is visible in the Fe–He axis. Only a few interstitial He atoms are trapped at the periphery of SIA clusters, as most

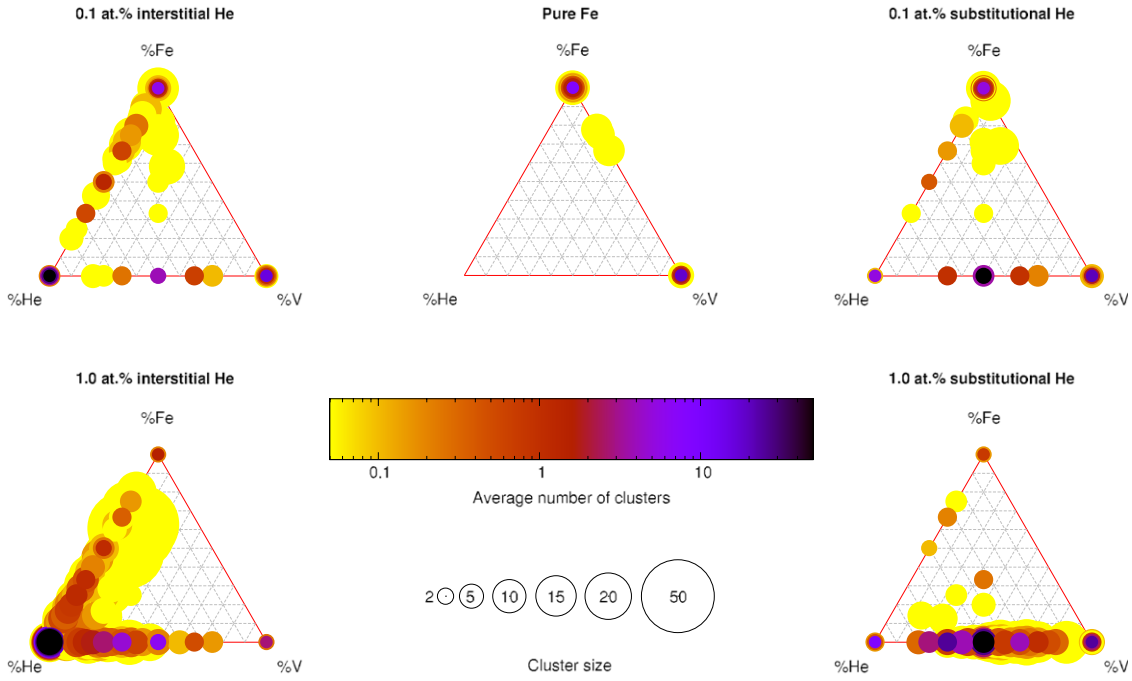

Figure 12. Ternary plots showing the average composition of the clusters remaining after 10 keV displacement cascades at 300 K for samples containing no helium, 0.1 at.% interstitial He and 0.1 at.% substitutional He. The size of each spot is proportional to the cluster size in number of defect species. The color scale gives the occurrence of clusters with the same composition.

of the helium remains trapped in small He_nV_m clusters. In this case, the homogeneous nucleation is favored. At higher content, the difference is abysmal. Indeed, with 1.0 at.% of substitutional He, very few SIA clusters remain after the cooling of the cascades. In fact, the SIAs formed in the early stages of the cascades are very likely to kick out a substitutional He from its location and recombine with the freed vacancy [28]. This mechanism is associated with a high energy gain [23] and leads to the formation of an interstitial He atom which can easily migrate and aggregate to an SIA cluster. In agreement with a previous study of Yang *et al* [14, 15], the increase in the amount of substitutional He leads to more numerous He_nV_m clusters nucleated directly in the displacement cascades.

Ternary plots reveal a line starting from the Fe corner and heading toward the middle of the He–V axis, cutting the ternary plots in half. This line, more visible for 0.1 at.% He content, corresponds to a few SIA clusters surrounded by He_nV_m clusters at their periphery with a n/m ratio close to 1. This situation, although less favorable than the trapping of He interstitials by SIA clusters, can also be explained by a non-negligible binding energy of around 0.3 eV on the loop edge and 0.6 eV on the loop plane [38]. The binding energy on the edge may be overcome at high temperature, leading to recombination of a substitutional He atom by a kick-out mechanism, which will end in a more favorable situation with an SIA cluster surrounded by an interstitial helium atom.

4.2. Fraction of glissile clusters

In pure iron, it has been shown that most SIA clusters formed during displacement cascades are mainly glissile, with SIAs aligned along ⟨111⟩ directions [36], with a fast 1D motion [39, 40]. The fraction of glissile clusters, i.e. having all their SIAs parallel relative to the ⟨111⟩ directions, was found to be around 70% and seemed poorly related to the PKA energy ⟨111⟩ directions [36]. The rest of the clusters are metastable sessile configurations, as their mobility is lowered by the presence of some SIAs oriented in ⟨110⟩, which locked those clusters. Temperature plays an important role in that it can flip these SIAs from ⟨110⟩ to ⟨111⟩ [41]. Depending on the study, these SIA clusters with SIAs oriented along ⟨111⟩ are normally favored when the number of SIAs contained in the cluster is greater than 3–5. This number depends on the method used for the calculation [42, 43]. Below this size the SIAs are preferentially oriented along the ⟨110⟩ direction, even at moderate temperatures [43].

Figure 13 shows the fraction of glissile clusters formed during displacement cascades for different initial helium contents at 10, 300 and 523 K. In this study clusters are considered to be glissile when they are constituted by SIAs whose orientation differs by less than 15° from a given ⟨111⟩ direction. The given fractions are the values averaged over all simulations carried out at 3, 7, 10 and 20 keV. In pure iron, the fraction of glissile clusters lies around 70% and tends to increase with increasing temperature. This result is consistent with calculations performed by Bacon *et al* [35, 36]. Adding 0.1 at.% of interstitial He does not seem to modify this tendency and similar fractions are found, even if this fraction is lower compared to pure iron at 300 K. With a higher content of interstitial He, the behavior changes drastically as the fractions are substantially reduced. In addition, a higher irradiation temperature clearly decreases this fraction. This effect can be related to the increase of the cluster size at

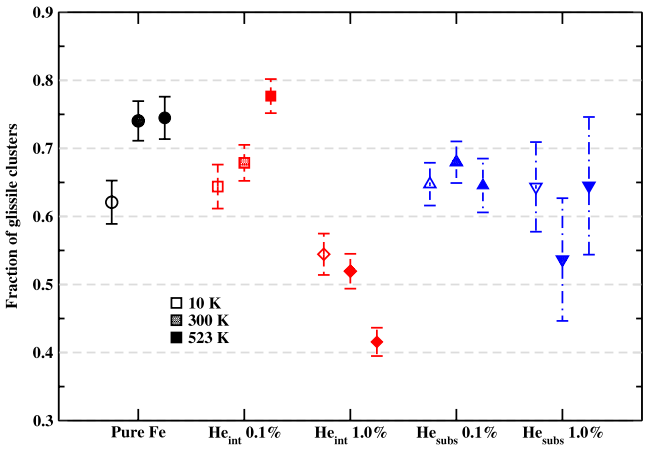

Figure 13. Fraction of glissile clusters formed during displacement cascades for different initial helium contents at 10, 300 and 523 K. The bars show the standard errors.

higher temperature, and yet larger clusters are easily found in a sessile configuration with non-parallel SIAs [35]. Moreover with this concentration of helium, a lot of SIA clusters formed are surrounded at their periphery by small He_nV_m clusters that actually perturb the orientation of the SIAs within the clusters. These SIAs would probably reorient themselves towards a ⟨111⟩ direction, but due to the timescale of our simulations a complete study of this phenomenon is beyond our scope. The presence of substitutional helium seems to decrease the fraction of glissile clusters to around 65% and 60%, for 0.1 at.% and 1.0 at.% helium content, respectively. Due to the large data scatter, no clear influence of irradiation temperature can be extracted from the results.

The presence of helium, in reducing the amount of glissile clusters, and consequently increasing the proportion of sessile clusters, would slow down the kinetics of annealing of the defects in α-iron. Indeed, a substantial amount of energy will be needed to reorient the sessile clusters to make them mobile. Only then could limited diffusion of SIA clusters decorated by helium occur.

4.3. Comparison with the Wilson–Johnson potential

Figure 14 gives the ternary plots resulting from 10 and 20 keV displacement cascades at 300 K for 0.1 at.% He interstitials in the case of the Juslin potential and Wilson–Johnson potential. Globally, no major differences are found concerning the composition of the clusters formed in both cases, and the two potentials seem to behave qualitatively in a similar manner. It should be noted that the most striking difference between these potentials is related to the difference in the position of the crossover in the dissociation energy curves of a helium atom and a vacancy from He_nV_m clusters. Indeed, with the Wilson–Johnson potential the optimal crossover is found around an n/m ratio of 1.8 with an associated dissociation energy of 3.6 eV [44, 45], to be compared to an n/m ratio close to 1.1 and a dissociation energy of 2.7 eV with the one we used. The impact of this feature on the cascades is visible in the ternary plots. A line highlighting an n/m ratio equal to 1 in the case of the Juslin potential, and equal to 2 in the case of the Wilson–Johnson potential, is observed. It is then clear that SIA clusters are more likely to be surrounded by small helium–vacancy clusters with a ratio closer to 1 with the Juslin potential, and closer to 2 with the Wilson–Johnson potential.

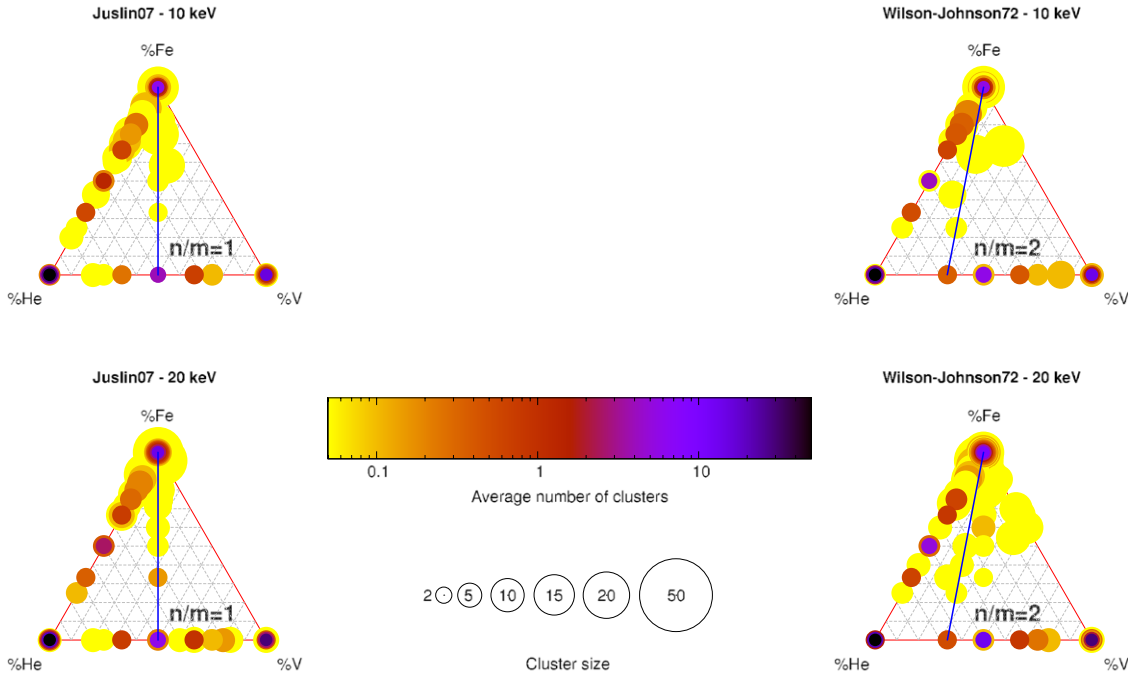

Figure 14. Average composition of the clusters remaining after 10 and 20 keV displacement cascades at 300 K for samples containing 0.1% of He interstitials using the Juslin potential [22] and Wilson–Johnson potential [24] to describe Fe–He interactions. The size of each spot is related to the cluster size in number of defect species. The color scale gives an indication of the occurrence of clusters with the same composition. The additional lines highlight particular n/m ratios within the ternary plots.

5. Summary

Molecular dynamics simulations have been carried out to study the effects of helium on displacement cascades in bcc iron. On the basis of our results, several findings can be given.

First of all, it is clear that the presence of helium plays a significant role in the damage production by influencing the number of generated defects but also their clustering. On the one hand, substitutional He atoms tend to decrease the number of Frenkel pairs produced within the cascade, playing the role of the source of vacancies easily available for the recombination with SIAs by a kick-out mechanism involving a substantial energy gain of around 4 eV. On the other hand, interstitial He atoms help the formation of SIAs by inducing an additional stress in the lattice, thus increasing the production of Frenkel pairs. Substitutional and interstitial helium atoms have thus an antagonist role which would occur simultaneously in a real material. The increase in helium concentration from 0.1 to 1.0 at.% exacerbates the observed effects.

Besides the production of defects, the presence of interstitial He atoms, and to a lesser extent with substitutional He atoms, favors the formation of SIA clusters during displacement cascades. Most of the large SIA clusters are found to be glissile and tend to form $\frac{1}{2}a_0\langle 111\rangle\{110\}$ dislocation loops. Their number and size clearly increase in the presence of helium compared to pure iron. This effect is easily explained by the high binding energy of interstitial He atoms with SIA clusters of about 1.2–1.4 eV. Substitutional He atoms have also non-negligible binding energies with SIA clusters but their reduced mobility leads to lesser effects. The strong binding energy and the very high mobility of interstitial He atoms lead then to the formation of SIA clusters which are surrounded at their periphery by small He_n clusters, located in the habit plane in the case of dislocation loops. SIA clusters appeared as heterogeneous nucleation sites for He bubbles. Our results show also He_nV_m nucleated at the periphery of the SIA clusters, with n/m ratios closer to 1. In the case of 1.0 at.% interstitial He, the helium density inside these He_nV_m clusters is higher. They could act as an additional source of self-interstitials for the growth of the SIA clusters by loop punching. Note that the He atoms or agglomerates attached to an SIA cluster should reduce its mobility. Also, at such a high helium content, a destructuration of the SIA cluster is observed, decreasing the glissile fraction. The diffusion of SIA clusters is thus expected to be significantly reduced by the surrounding helium atoms.

Some small helium–vacancy clusters are homogeneously nucleated within displacement cascades. The helium-to-vacancy ratios in the He_nV_m clusters tend to be above 1 in the presence of interstitial He and closer to 1 in the presence of substitutional He. The larger He_nV_m clusters are found in the latter case for ratios below 1.

Our results also show that irradiation temperature plays a major role in the defect production and the clustering in the presence of helium. Due to the higher defect mobility at higher temperature, especially the one of interstitial He atoms, the effects of helium are globally enhanced with increasing temperature. In the substitutional He cases, some interstitial He atoms are generated during the displacement cascades. At low irradiation temperature, their mobility is reduced. As a consequence, an increase in size of SIA clusters is not observed at 10 K as the interstitial He atoms do not have the time to reach SIA clusters to stabilize them, at least on the timescale of our simulations. At 300 and 523 K, the diffusion of interstitial He atoms is fast enough to reach and stabilize SIA clusters that can further grow.

Our study shows that helium atoms are efficient traps for SIA clusters, and could thus be at the origin of traps added in KMC simulations to reproduce experimental data. In this perspective, a systematic study of the binding energies between helium atoms and SIA clusters, and their migration energies, would be useful.

Acknowledgments

We thank M J Caturla for useful discussions. This work, supported by the European Communities under the contract of Association between EURATOM and Confédération Suisse, was carried out within the framework of the European Fusion Development Agreement. The views and opinions expressed herein do not necessarily reflect those of the European Commission. The Paul Scherrer Institute is acknowledged for the overall use of its facilities.

References

[1] Yamamoto T, Odette G R, Kishimoto H, Rensman J-W and Miaoa P 2006 *J. Nucl. Mater.* **356** 27
[2] Vassen R, Trinkaus H and Jung P 1991 *Phys. Rev.* B **44** 4206
[3] Ishiyama Y, Kodama M, Yokota N, Asano K, Kato T and Fukuya K 1996 *J. Nucl. Mater.* **239** 90
[4] Trinkaus H and Singh B N 2003 *J. Nucl. Mater.* **323** 229
[5] Victoria M, Dudarev S, Boutard J L, Diegele E, Lässer R, Almazouzi A, Caturla M J, Fu C C, Källne J, Malerba L, Nordlund K, Perlado M, Rieth M, Samaras M, Schaeublin R, Singh B N and Willaime F 2007 *Fusion Eng. Des.* **82** 2413
[6] Malerba L 2006 *J. Nucl. Mater.* **351** 28
[7] Dauben P, Wahi R P and Wollenberger H 1986 *J. Nucl. Mater.* **141** 723
[8] Ghoniem N M 1990 *J. Nucl. Mater.* **174** 168
[9] Trinkaus H 2003 *J. Nucl. Mater.* **318** 234
[10] Fu C-C and Willaime F 2005 *Phys. Rev.* B **72** 064117
[11] Heinisch H L, Gao F and Kurtz R J 2007 *J. ASTM Int.* **4** 100946
[12] Caturla M J and Ortiz C J 2007 *J. Nucl. Mater.* **362** 141
[13] Domain C, Becquart C S and Malerba L 2004 *J. Nucl. Mater.* **335** 121
[14] Yang L, Zu X T, Xiao H Y, Gao F, Heinisch H L, Kurtz R J and Liu K Z 2006 *Appl. Phys. Lett.* **88** 091915
[15] Yang L, Zu X T, Xiao H Y, Gao F, Liu K Z, Heinisch L, Kurtz R J and Yang S Z 2006 *Mater. Sci. Eng.* A **427** 343
[16] Yu J, Yu G, Yao Z and Schäublin R 2007 *J. Nucl. Mater.* **367** 462
[17] Ehrlich K 1999 *Phil. Trans. R. Soc.* A **357** 595
[18] Diaz de la Rubia T and Guinan M W 1990 *J. Nucl. Mater.* **174** 151
[19] Lucas G and Schäublin R 2008 *J. Nucl. Mater.* at press
[20] Ackland G J, Bacon D J, Calder A F and Harry T 1997 *Phil. Mag.* A **75** 713
[21] Beck D E 1968 *Mol. Phys.* **14** 311
[22] Juslin N and Nordlund K 2008 *J. Nucl. Mater.* at press doi:10.1016/j.jnucmat.2008.08.029

[23] Fu C-C and Willaime F 2007 *J. Nucl. Mater.* **367** 244
[24] Wilson W D and Johnson R D 1972 *Interatomic Potentials and Simulation of Lattice Defects* (New York: Plenum) chapter (Rare Gases in Metals) p 375
[25] Allen M P and Tildesley D J 1987 *Computer Simulation of Liquids* (New York: Oxford Science)
[26] Souidi A, Becquart C S, Domain C, Terentyev D, Malerba L, Caldere A F, Bacon D J, Stoller R E, Osetsky Y N and Hou M 2006 *J. Nucl. Mater.* **355** 89
[27] Bacon D J, Calder A F and Gao F 1997 *J. Nucl. Mater.* **251** 1
[28] Gösele U, Frank W and Seeger A 1980 *Appl. Phys.* **23** 361
[29] Martin G 1984 *Phys. Rev.* B **30** 1424
[30] Martin G and Bellon P 1987 *Mater. Sci. Forum* **15–18** 1337
[31] Brinkman J A 1954 *J. Appl. Phys.* **25** 961
[32] Souidi A, Hou M, Becquart C S and Domain C 2001 *J. Nucl. Mater.* **295** 179
[33] Ventelon L, Wirth B and Domain C 2006 *J. Nucl. Mater.* **351** 119
[34] Arakawa K, Ono K, Isshiki M, Mimura K, Uchikoshi M and Mori H 2007 *Science* **318** 956
[35] Bacon D J, Gao F and Osetsky Y N 2000 *J. Nucl. Mater.* **276** 1
[36] Bacon D J, Osetsky Yu N, Stollerb R and Voskoboinikov R E 2003 *J. Nucl. Mater.* **323** 152
[37] Schäublin R and Chiu Y L 2007 *J. Nucl. Mater.* **362** 152
[38] Shim J-H, Kwon S C, Kim W W and Wirth B D 2007 *J. Nucl. Mater.* **367** 292
[39] Wirth B D, Odette G R, Maroudas D and Lucas G E 1997 *J. Nucl. Mater.* **244** 185
[40] Osetsky Yu N, Bacon D J, Serra A, Singh B N and Golubov S I 2003 *Phil. Mag.* **83** 61
[41] Terentyev D A, Malerba L and Hou M 2007 *Phys. Rev.* B **75** 104108
[42] Willaime F, Fu C C, Marinica M C and Dalla Torre J 2005 *Nucl. Instrum. Methods Phys. Res.* B **228** 92
[43] Marinica M-C and Willaime F 2007 *Solid State Phenom.* **129** 67
[44] Morishita K, Sugano R and Wirth B D 2003 *J. Nucl. Mater.* **323** 243
[45] Morishita K, Sugano R, Wirth B D and Diaz de la Rubia T 2003 *Nucl. Instrum. Methods Phys. Res.* B **202** 76